Exactly solvable mixed-spin Ising-Heisenberg diamond chain with biquadratic interactions and single-ion anisotropy

Onofre Rojas,[1,*] S. M. de Souza,[1] Vadim Ohanyan,[2,3,†] and Martiros Khurshudyan[2]

[1]*Departamento de Ciencias Exatas, Universidade Federal de Lavras, CP 3037, 37200000, Lavras, MG, Brazil*

[2]*Yerevan State University, A. Manoogian, 1, Yerevan, 0025 Armenia*

[3]*Yerevan Physics Institute, Alikhanian Br. 2, Yerevan, 0036, Armenia*

(Received 14 August 2010; revised manuscript received 1 February 2011; published 29 March 2011)

An exactly solvable variant of a mixed spin-(1/2,1) Ising-Heisenberg diamond chain is considered. Vertical spin-1 dimers are taken as quantum ones with Heisenberg bilinear and biquadratic interactions and with single-ion anisotropy, while all interactions between spin-1 and spin-1/2 residing on the intermediate sites are taken in the Ising form. The detailed analysis of the $T = 0$ ground-state phase diagram is presented. The phase diagrams have been shown to be rather rich, demonstrating a large variety of ground states: a saturated one, three ferrimagnetic ones with magnetization equal to 3/5, and another four ferrimagnetic ground states with magnetization equal to 1/5. There are also two frustrated macroscopically degenerated ground states that could exist at zero magnetic filed. Solving the model exactly within a classical transfer-matrix formalism we obtain exact expressions for all thermodynamic functions of the system. The thermodynamic properties of the model have been described exactly by exact calculation of the partition function within the direct classical transfer-matrix formalism.

DOI: 10.1103/PhysRevB.83.094430 PACS number(s): 75.10.Hk, 75.10.Jm

I. INTRODUCTION

Lattice models of quantum magnetism continue to be the focus of attention of theoretical condensed matter physicists. Besides being of great practical importance connected with the description of magnetic and thermodynamic properties of real magnetic materials, this research area is also attractive from the general statistical mechanics and strongly correlated system theory points of view, especially when one deals with an exactly solvable strongly interacting many-body system. The diamond chain is a one-dimensional lattice spin system in which the vertical spin dimers alternate with single spins (see Fig. 1). This model with $S = 1/2$ is believed to describe the magnetic lattice of the mineral azurite, $Cu_3(CO_3)_2(OH)_2$, which is famous for its deep blue pigmentation.[1–4] Theoretical research on various aspects of diamond chain physics has received much attention during recent years.[5–16] Diamond chain and especially diamond chain with mixed $(S,S/2)$ spin are shown to have very rich ground-state phase diagrams with Haldane and several spin-cluster states, which are a tensor product of exact local eigenstates of cluster spins.[5,6] Many other issues of diamond chain physics have been investigated theoretically during recent years including Dzyaloshinskii-Moriya term influence on magnetization processes,[7] multiple-spin-exchange effects,[8] magnetization plateaus,[9,10] magnetocaloric effect,[11] etc. Very recently another interesting feature of diamond chains, the possibility of localized magnon excitations, also has been investigated.[12]

An especially important issue is the effect of frustration, which is rather strong in an antiferromagnetic diamond chain because of triangular arrangement of the sites. Variants of frustrated recurrent lattices with a diamond plaquette have been studied in Refs. 17 and 18. However, a diamond chain is not integrable in general. Thus, the exact analysis of the dynamic and especially thermodynamic properties of a diamond chain is a very complicated issue. Nevertheless, one can consider various exactly solvable variants of spin systems possessing a diamond chain topology of interaction bonds with a simplified structure of interactions.[13–16] The diamond chain with only an Ising type of interaction has been exactly solved within classical transfer-matrix technique in Ref. 13, revealing the rich structure of a $T = 0$ ground-state phase diagram. Yet other exactly solvable diamond chains have been considered in Refs. 14–16,19, where vertical spin dimers have been taken as quantum ones with XXZ interaction, while interaction between spins localized on vertical dimer sites and spins from the single sites alternating with them is of an Ising type. Mapping the system into a single Ising chain within iteration-decoration transformation,[20–22] the authors gave a complete description of the ground-state properties, a $T = 0$ ground-state phase diagram, as well as thermodynamic functions for all values of vertical dimer spins magnitude S. In a very recent paper the diamond chain with XX interaction has been considered in the Jordan-Wigner formalism.[19]

Considering the mixed-spin chains (or other one-dimensional spin systems with more complicated geometry) with Ising and Heisenberg bonds (or even just Ising counterparts of the known quantum spin models) one can achieve a twofold goal: to construct an exactly solvable lattice spin model that allows one to obtain an analytic expression for all thermodynamic functions of the model, and to get approximate models that can be useful for understanding the properties of underlying purely quantum models.[14–16,23–29] Exact thermodynamic solutions of such models even can shed light on the properties of real magnetic materials. For instance, for alternating spin chains, even the simplest models with only an Ising interaction can reflect the underlying magnetic behavior of the corresponding Heisenberg counterpart at least in a qualitative way;[30,31] moreover, some exactly solvable models with Ising and Heisenberg bonds can also provide a satisfactory quantitative picture.[29] Very recently, the synthesis of the novel class of trimetalic $3d$-$4d$-$4f$ coordination polymers has been reported. One of them, a one-dimensional coordination polymer compound containing $3d$ (Cu^{2+}), $4d$ (Mo^{5+}), and

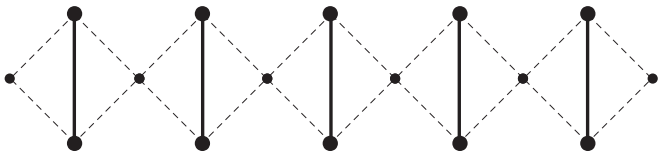

FIG. 1. The diamond chain with Ising and Heisenberg bonds. Solid bold lines denote XXZ quantum bonds; dotted lines correspond to Ising interactions. Large (small) circles denote $\mathbf{S}$ (σ) spins.

$4f$ (Dy^{3+}) ions, is shown to exhibit the properties of a one-dimensional magnet with Ising and Heisenberg bonds.[32,33] The appearance of Ising interactions between magnetic ions in this compound is connected with the extremely anisotropic properties of Dy^{3+} ground states ($g_{\parallel} = 19.6$, $g_{\perp} \approx 0$). Thus, the interactions of Dy^{3+} with the surrounding Cu^{2+} and Mo^{5+} ions are, to the great extent, of Ising type, involving spin projection along the dysprosium anisotropy axis, while the interaction bonds Cu^{2+}—Mo^{5+} correspond to Heisenberg interaction.[32,33] Recently, the theoretical calculations of the magnetic properties of the corresponding coordination polymer compound have been performed in Ref. 33 using the transfer matrix method. Though the aforementioned one-dimensional coordination polymer system is not exactly the Ising-Heisenberg diamond chain considered in the present paper, this discovery of novel classes of magnetic materials makes the investigation of exact solutions of spin chains with Ising and Heisenberg bonds important from a practical point of view as well.

In this paper we consider mixed spin-(1,1/2) diamond chain with Ising and Heisenberg bonds that extends the system considered in Ref. 16 by including a biquadratic term for $S = 1$ XXZ dimers and single-ion anisotropy. Biquadratic terms are usually originated from the spin-lattice coupling in the adiabatic phonons approximation[34] but also can be considered as the effect of quadrupole interaction between the spins. We do not make any assumption about the origin of biquadratic terms, considering them as a part of the general Hamiltonian. The model allows one to calculate the partition function and, thus, all thermodynamic quantities exactly within classical transfer-matrix formalism.[35] We present the analysis of $T = 0$ ground-state phase diagrams and plot the curves of magnetization processes for finite temperatures, demonstrating magnetization plateaus at $M = 1/5$ and $3/5$ in the units of saturation magnetization.

The paper is organized as follows. In Sec. II we formulate the model and present its eigenvalues. In Sec. III we describe possible ground states of the system and present the ground-state phase diagram. In Sec. IV we present its exact solution and discuss the magnetization and thermodynamics properties of the model. Finally in Sec. V a short summary is given.

II. THE MODEL AND ITS EXACT SOLUTION

Let us consider the system of vertical $S = 1$ spin dimers with Heisenberg XXZ bilinear and biquadratic interactions and uniaxial single-ion anisotropy. These dimers are assembled to the chain by alternating with Ising spins σ, so that each spin S in a certain dimer interacts to both its left and right Ising spins via an Ising-type interaction (see Fig. 1). So we have the so-called diamond chain with $S = 1$ Heisenberg dimers and $\sigma = 1/2$ Ising spins between them. The corresponding Hamiltonian is the sum over the block Hamiltonians:

$$\mathcal{H} = \sum_{i=1}^{N} \left[\mathcal{H}_i - \frac{h_2}{2}(\sigma_i + \sigma_{i+1}) \right],$$
$$\mathcal{H}_i = J(\mathbf{S}_{i1} \cdot \mathbf{S}_{i2})_{\Delta} + K(\mathbf{S}_{i1} \cdot \mathbf{S}_{i2})_{\Delta}^2 + D\left[\left(S_{i1}^z\right)^2 + \left(S_{i2}^z\right)^2 \right]$$
$$+ J_0(\sigma_i + \sigma_{i+1})\left(S_{i1}^z + S_{i2}^z\right) - h_1\left(S_{i1}^z + S_{i2}^z\right), \qquad (1)$$

where N is the number of the unit cells (blocks with two spin-1 and one spin-1/2), while i corresponds to the particles at the i-cell. J is the coupling constant of bilinear XXZ interaction between Heisenberg spins, which we assume to be of the following form:

$$(\mathbf{S}_{i1} \cdot \mathbf{S}_{i2})_{\Delta} = \Delta\left(S_{i1}^x S_{i2}^x + S_{i1}^y S_{i2}^y\right) + S_{i1}^z S_{i2}^z, \qquad (2)$$

whereas K denotes the biquadratic XXZ interaction term, D means the single-ion anisotropy, and J_0 is the purely Ising interaction term. Here h_2 and h_1 are the external magnetic field acting on σ_i and S_i respectively.

In order to solve this model, first, we need to diagonalize the block Hamiltonian for arbitrary ith block. Nine eigenvalues of $\mathcal{H}_i$, $\lambda_n(\sigma_i, \sigma_{i+1})$, $n = 1, \ldots, 9$ can be found analytically, which can be written as

$$\lambda_{1,2} = J + K + 2D \pm 2[-h_1 + J_0(\sigma_i + \sigma_{i+1})],$$
$$\lambda_{3,4} = \Delta(J + \Delta K) + D \pm [-h_1 + J_0(\sigma_i + \sigma_{i+1})],$$
$$\lambda_{5,6} = -\Delta(J - \Delta K) + D \pm [-h_1 + J_0(\sigma_i + \sigma_{i+1})], \qquad (3)$$
$$\lambda_7 = -J + K + 2D,$$
$$\lambda_{8,9} = \frac{-J + (1 + 4\Delta^2)K + 2D}{2} \pm \frac{1}{2}R,$$

where for simplicity R denotes the following expression:

$$R = \sqrt{8\Delta^2(J - K)^2 + (J - K - 2D)^2}. \qquad (4)$$

The eigenvectors of block Hamiltonian $\mathcal{H}_i$ up to the inversion of all spins are

$$|v_2\rangle = |1,1\rangle, \quad \Rightarrow \quad \lambda_1, \lambda_2,$$
$$|v_{1,s}\rangle = \frac{1}{\sqrt{2}}(|1,0\rangle + |0,1\rangle), \quad \Rightarrow \lambda_3, \lambda_4,$$
$$|v_{1,a}\rangle = \frac{1}{\sqrt{2}}(-|1,0\rangle + |0,1\rangle), \quad \Rightarrow \lambda_5, \lambda_6, \qquad (5)$$
$$|v_{0,a}\rangle = \frac{1}{\sqrt{2}}(-|-1,1\rangle + |1,-1\rangle), \quad \Rightarrow \lambda_7,$$
$$|v_{0,\pm}\rangle = \frac{1}{\sqrt{2 + c_{\pm}^2}}(|-1,1\rangle + c_{\pm}|0,0,\rangle + |1,-1\rangle), \quad \Rightarrow \lambda_8, \lambda_9,$$

where 1, 0, and -1 in first (second) place stand for the $S^z = 1$, 0, and -1 states for first (second) spin in vertical dimer, and the following notation is adopted:

$$c_{\pm} = \frac{1}{2\Delta}\left(1 + \frac{2D \pm R}{K - J}\right). \qquad (6)$$

The first eigenvectors of the dimer defined as $|v_2\rangle$ correspond to the parallel ordered spins with magnetization per site $m_s = 1$, the eigenvector $|v_{1,s}\rangle$ and $|v_{1,a}\rangle$ corresponds to symmetric and antisymmetric state vector, respectively, whereas

$|v_{0,a}\rangle$ is an antisymmetric state vector with magnetization $m_s = 0$; finally, $|v_{0,\pm}\rangle$ are the symmetric eigenvectors with magnetization $m_s = 0$.

The remaining eigenvectors of the eigenvalues λ_2, λ_4, and λ_6 can be obtained using the spin inversion.

A. Special case $K = J$

At the special value $K = J$ the $S^z_{\rm tot} = 0$ sector of the block Hamiltonian undergoes qualitative changes that can be obtained by substituting carefully the $K = J$ value into the general solution presented in Eq. (5). This should be considered as a consequence of the special symmetry of the Hamiltonian for these values of parameters, more precisely, the fact that the operator $(\mathbf{S}_1 \cdot \mathbf{S}_2)_\Delta + (\mathbf{S}_1 \cdot \mathbf{S}_2)^2_\Delta$ can be represented in terms of permutation operators P_{12}. In this case the eigenstates $|v_{0,a}\rangle$ and $|v_{0,\pm}\rangle$ of the Hamiltonian reduce to the following ones:

$$\begin{aligned} |v_{0,a}\rangle &= \frac{1}{\sqrt{2}}(|1,-1\rangle - |-1,1\rangle), \quad \Rightarrow \lambda_7 = 2D, \\ |v_{0,+}\rangle &= |0,0\rangle, \quad \Rightarrow \lambda_8 = 2J\Delta^2, \\ |v_{0,-}\rangle &= \frac{1}{\sqrt{2}}(|1,-1\rangle + |-1,1\rangle), \quad \Rightarrow \lambda_9 = 2(J\Delta^2 + D). \end{aligned} \tag{7}$$

Note that a straightforward substitution in Eq. (6) could yield an undefined coefficient of the eigenstates.

III. GROUND-STATE PHASE DIAGRAMS

Let us describe the possible $T = 0$ ground states of the chain under consideration and the corresponding energies per block. Generally speaking, there are $9 \times 2 = 18$ possible ground states for each block. However, if one restricts one's self to the ground states that are equivalent up to the inversion of all spins, one will arrive at the following spin configurations. The fully polarized state ($M = 1$) is

$$|\mathrm{SP}\rangle = \prod_{i=1}^{N} |v_2\rangle_i \otimes |\uparrow\rangle_i, \quad \varepsilon_{\rm SP} = J + K + 2D + 2J_0 - \frac{5}{2}H, \tag{8}$$

where $|\uparrow\rangle_i (|\downarrow\rangle_i)$ stands for the up(down) state of the σ spin in the ith block. Hereafter, we also put $h_1 = h_2 = H$. The next sector of ground states contains three different ferrimagnetic spin configurations with the value of magnetization equal to 3/5 ($M = 3/5$):

$$\begin{aligned} |\mathrm{F1}\rangle &= \prod_{i=1}^{N} |v_2\rangle_i \otimes |\downarrow\rangle_i, \quad \varepsilon_{\rm F1} = J + K + 2D - 2J_0 - \frac{3}{2}H, \\ |\mathrm{F2}\rangle &= \prod_{i=1}^{N} |v_{1,s}\rangle_i \otimes |\uparrow\rangle_i, \\ \varepsilon_{\rm F2} &= \Delta(J + \Delta K) + D + J_0 - \frac{3}{2}H, \\ |\mathrm{F3}\rangle &= \prod_{i=1}^{N} |v_{1,a}\rangle_i \otimes |\uparrow\rangle_i, \\ \varepsilon_{\rm F3} &= -\Delta(J - \Delta K) + D + J_0 - \frac{3}{2}H. \end{aligned} \tag{9}$$

There are also another four ferrimagnetic ground states with $M = 1/5$:

$$\begin{aligned} |\mathrm{F4}\rangle &= \prod_{i=1}^{N} |v_{1,s}\rangle_i \otimes |\downarrow\rangle_i, \\ \varepsilon_{\rm F4} &= \Delta(J + \Delta K) + D - J_0 - \frac{1}{2}H, \\ |\mathrm{F5}\rangle &= \prod_{i=1}^{N} |v_{1,a}\rangle_i \otimes |\downarrow\rangle_i, \\ \varepsilon_{\rm F5} &= -\Delta(J - \Delta K) + D - J_0 - \frac{1}{2}H, \\ |\mathrm{F6}\rangle &= \prod_{i=1}^{N} |v_{0,a}\rangle_i \otimes |\uparrow\rangle_i, \\ \varepsilon_{\rm F6} &= -J + K + 2D - \frac{1}{2}H, \\ |\mathrm{F7}\rangle &= \prod_{i=1}^{N} |v_{0,-}\rangle_i \otimes |\uparrow\rangle_i, \\ \varepsilon_{\rm F7} &= \frac{1}{2}[-J + (1 + 4\Delta^2)K + 2D - R] - \frac{1}{2}H. \end{aligned} \tag{10}$$

When no external magnetic field is applied, there is also the possibility of frustrated ground-state formation, in which the orientation of σ spins in each block is not defined. In this case all σ spins become decoupled and behave like free spins. There are two frustrated ground states:

$$\begin{aligned} |\mathrm{FR1}\rangle &= \prod_{i=1}^{N} |v_{0,a}\rangle_i \otimes |\xi\rangle_i, \quad \varepsilon_{\rm FR1} = -J + K + 2D, \\ |\mathrm{FR2}\rangle &= \prod_{i=1}^{N} |v_{0,-}\rangle_i \otimes |\xi\rangle_i, \\ \varepsilon_{\rm FR2} &= \frac{1}{2}[-J + (1 + 4\Delta^2)K + 2D - R]. \end{aligned} \tag{11}$$

Here $|\xi\rangle_i$ stands for an arbitrary value of the σ spin in the ith block. Thus, for $H = 0$ if the $S = 1$ dimer has $S^z_{\rm tot} = 0$, then its neighboring σ spins become decoupled, which results in macroscopic nonzero entropy $S/N = \log 2$ for each of the frustrated ground states of Eq. (11). Applying a magnetic field one removes the twofold macroscopic degeneracy driving $|\mathrm{FR1}\rangle$ and $|\mathrm{FR2}\rangle$ ground states into $|\mathrm{F6}\rangle$ and $|\mathrm{F7}\rangle$, respectively. Nevertheless, in some papers the two last nondegenerated ground states of Eqs. (10) are mentioned as frustrated ones.[14–16]

Hereafter, to discuss the phase diagrams we will consider the external magnetic field as $h_1 = h_2 = H$. It is also convenient to present all parameters as units of $|J|$. Thus, we define $\kappa = K/|J|$, $j_0 = J_0/|J|$, $\delta = D/|J|$, and $h = H/|J|$. In Fig. 2 one can see four ground-state phase diagrams plotted in the (κ,h) plane demonstrating a vast variety of ground states for fixed values of δ and j_0. These plots summarize the effect of the biquadratic term. The equations of phase boundaries for $J > 0$, $\Delta = 2$, $j_0 = 0.5$, and $\delta = 0.5$ [Fig. 2(a)] are

$$\begin{aligned} &\text{between F7 and SP,} \quad h = \tfrac{1}{4}[6 - 15\kappa + \sqrt{\kappa^2 + 32(\kappa - 1)^2}], \\ &\text{between F7 and F3,} \quad h = \tfrac{1}{2}[-2 - 9\kappa + \sqrt{\kappa^2 + 32(\kappa - 1)^2}], \\ &\text{between F3 and SP,} \quad h = 4 - 3\kappa. \end{aligned} \tag{12}$$

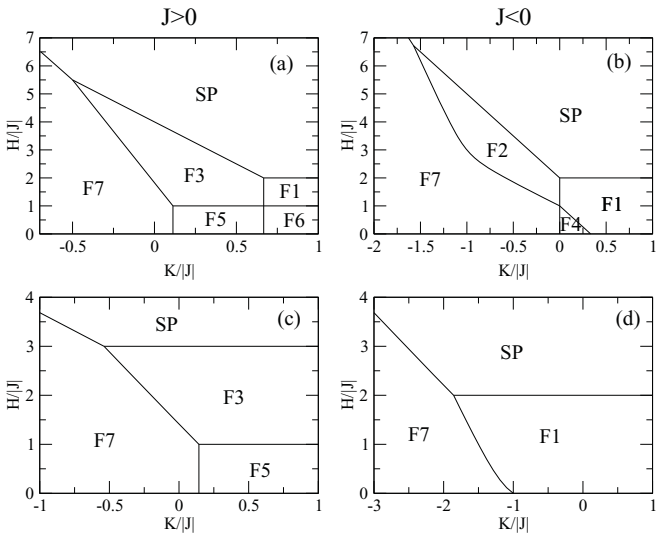

FIG. 2. Ground-state phase diagrams in the (κ,h) plane demonstrating the effect of a biquadratic term. Here $\kappa = K/|J|$ and $h = H/|J|$. The values of all other parameters, $j_0 = J_0/|J|$, $\delta = D/|J|$, are fixed as follows: $j_0 = 1/2, \delta = 1/2$. Left panels (a) and (c) correspond to the antiferromagnetic Heisenberg interaction $J > 0$; right panels (b) and (d) to the ferromagnetic one $J < 0$. In upper panels (a) and (b) $\Delta = 2$ has been taken, while in lower panels (c) and (d) one can see phase diagrams for the isotropic case $\Delta = 1$. At $H = 0$ the F6 and F7 ground states in all four panels passed to the corresponding frustrated phases FR1 and FR2, respectively. So the lines corresponding to $H = 0$ ground states below F6 and F7 should be understood as belonging to frustrated ground states corresponding to disordered configuration of σ spins.

The rest of the phase boundaries in this case are either horizontal or vertical lines in the (κ, h) plane. F5 and F3 as well as F6 and F1 are separated by the $h = 1$ line, while the phase boundary between F5 and F6 as well as between F3 and F1 is the vertical line situated at $\kappa = 2/3$. Ground states F7 and F5 are separated by the line $\kappa = 1/12(-17 + \sqrt{337}) \approx 0.113\,13$.

For the case of antiferromagnetic Heisenberg interaction between $S = 1$ spin ($J < 0$) presented in Fig. 2(b) the equations of the phase boundaries are

$$\begin{gathered}\text{between F7 and SP,}\\ h = \tfrac{1}{4}[-15\kappa + \sqrt{32(\kappa+1)^2 + (\kappa+2)^2}],\\ \text{between F7 and F2,}\\ h = \tfrac{1}{2}[-4 - 9\kappa + \sqrt{32(\kappa+1)^2 + (\kappa+2)^2}],\\ \text{between F2 and SP,}\quad h = 2 - 3\kappa,\\ \text{between F4 and F1,}\quad h = 1 - 3\kappa.\end{gathered} \tag{13}$$

The boundary between F1 and saturated ground state SP is the straight line $h = 2$. Horizontal line $\kappa = 0$ separates F4 and F7 as well as F1 and F2. In order to demonstrate the significant role of exchange anisotropy Δ we plotted also the ground-state phase diagrams for the isotropic case $\Delta = 1$ [Fig. 2(c) and 2(d)] for antiferromagnetic and ferromagnetic J, respectively. One can see the simplification of the ground-state phase diagram via the disappearance of two ground states presented in the anisotropic case $\Delta = 2$ [Fig. 2(a) and 2(b)]. So for $J > 0$ one can find, besides SP, only F3, F5, and F7 and for $J < 0$ only F1 and F7 ground states, respectively. The equation of phase boundaries for antiferromagnetic J, isotropic $\Delta = 1$, and $j_0 = 0.5$, $\delta = 0.5$ are

$$\begin{gathered}\text{between F7 and SP,}\\ h = \tfrac{1}{4}[6 - 3\kappa + \sqrt{8(\kappa-1)^2 + \kappa^2}],\\ \text{between F7 and F3,}\\ h = \tfrac{1}{2}[-\kappa + \sqrt{8(\kappa-1)^2 + \kappa^2}].\end{gathered} \tag{14}$$

Ground states F3 and SP are separated by the horizontal line $h = 3$; another two straight lines appear between F3 and F5 and F7 and F5 at $h = 1$ and $\kappa = 1/7$, respectively. In the case of ferromagnetic J and the isotropic exchange interaction presented in Fig. 2(d) one can see only three possible ground states: F1, F7, and SP. Here the horizontal line $h = 2$ separates F1 and SP, while other two phase boundaries are given by

$$\begin{gathered}\text{between F7 and SP,}\\ h = \tfrac{1}{4}[6 - 3\kappa + \sqrt{8(\kappa+1)^2 + \kappa^2}],\\ \text{between F7 and F1,}\\ h = \tfrac{1}{2}[2 - 3\kappa + \sqrt{8(\kappa+1)^2 + \kappa^2}].\end{gathered} \tag{15}$$

In order to summarize the effects of the Ising coupling J_0 we plotted two other ground-state phase diagrams presented in Fig. 3. Here the left panel shows ground-state boundaries in the (j_0, h) plane for fixed values of δ, κ, and Δ, while the right panel demonstrates the phase boundaries for fixed δ,h, and Δ in the (κ,j_0) plane. For the sake of brevity we just list the equation of phase boundaries. For the left panel:

$$\begin{gathered}\text{between F3 and SP,}\quad h = \frac{23}{8} + j_0,\\ \text{between F3 and F7,}\quad h = \frac{1}{2}\left(\frac{\sqrt{11}}{2} - \frac{3}{4}\right) + j_0,\\ \text{between F3 and F5,}\quad h = 2j_0,\end{gathered}$$

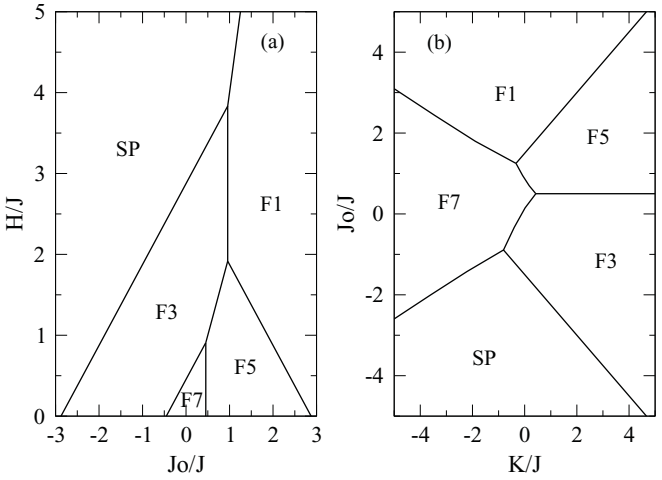

FIG. 3. Ground-state phase diagrams demonstrating the influence of J_0. Here $\Delta = 1/2$ and $\delta = 1$. (a) The ground-state phase diagram in the (j_0,h) plane for a fixed value of biquadratic interaction $\kappa = 1/2$; (b) the ground-state phase diagram in the (κ, j_0) plane for a fixed value of magnetic field $h = 1$.

$$\begin{aligned}
&\text{between F5 and F1,} \quad h = \frac{23}{8} - j_0, \\
&\text{between F1 and SP,} \quad h = 4j_0, \\
&\text{between F7 and F5,} \quad j_0 = \frac{1}{2}\left(\frac{\sqrt{11}}{2} - \frac{3}{4}\right), \\
&\text{between F3 and F1,} \quad j_0 = \frac{23}{24}.
\end{aligned} \tag{16}$$

For right panel:

$$\begin{aligned}
&\text{between F7 and SP,} \\
&j_0 = -\frac{1}{4}[1 + \sqrt{2(\kappa-1)^2 + (\kappa+1)^2}], \\
&\text{between F7 and F3,} \\
&j_0 = \frac{1}{2}\left[2 - \frac{3}{2}\kappa - \sqrt{2(\kappa-1)^2 + (\kappa+1)^2}\right], \\
&\text{between F7 and F5,} \\
&j_0 = \frac{1}{2}\left[-\frac{3}{2}\kappa + \sqrt{2(\kappa-1)^2 + (\kappa+1)^2}\right], \\
&\text{between F7 and F1,} \\
&j_0 = \frac{1}{4}[3 + \sqrt{2(\kappa-1)^2 + (\kappa+1)^2}], \\
&\text{between SP and F3,} \quad j_0 = -\frac{3}{2}\left(1 + \frac{1}{2}\kappa\right), \\
&\text{between F3 and F5,} \quad j_0 = \frac{1}{2}, \\
&\text{between F5 and F1,} \quad j_0 = \frac{3}{2}\left(1 + \frac{1}{2}\kappa\right).
\end{aligned} \tag{17}$$

Another two ground-state phase diagrams demonstrating the influence of single-ion anisotropy are presented in Fig. 4. The left (right) panel exhibits phase boundaries for $h = 1$, $j_0 = 1$, and $\Delta = 0.5$ ($\kappa = 0.5$), respectively. The phase boundaries for the left [in the (δ,κ) plane] and right [in the (δ,Δ) plane] panels, respectively, are

$$\begin{aligned}
&\text{between F1 and F7,} \quad \delta = -\frac{3(2 + 2\kappa - \kappa^2)}{4(2+\kappa)}, \\
&\text{between F1 and F5,} \quad \delta = \frac{1}{4}(2 - \kappa), \\
&\text{between F5 and F7,} \\
&\delta = \frac{1}{2}(1 - \kappa + \sqrt{2 + 10\kappa + 1/4\kappa^2}),
\end{aligned} \tag{18}$$

and

$$\text{between F1 and F4,} \quad \delta = \tfrac{1}{2}(\Delta + 1)^2, \tag{19}$$

$$\text{between F1 and F5,} \quad \delta = \tfrac{1}{2}(\Delta - 1)^2,$$

$$\begin{aligned}
&\text{between F7 and F4,} \\
&\delta = \tfrac{1}{2}(1/2 - \sqrt{9/4 + \Delta^4 - 4\Delta^3 + 5\Delta^2 - 6\Delta}),
\end{aligned} \tag{20}$$

$$\begin{aligned}
&\text{between F7 and F5,} \\
&\delta = \tfrac{1}{2}(1/2 + \sqrt{9/4 + \Delta^4 + 4\Delta^3 + 5\Delta^2 + 6\Delta}).
\end{aligned}$$

Finally, the zero-field ground-state phase diagram is presented in Fig. 5. The phase diagram exhibits the appearance of two frustrated ground states at a zero magnetic field. We choose $\delta = 0$ and a rather small value of biquadratic interactions $\kappa = 0.1$. The equations for the phase boundaries are

$$\begin{aligned}
&\text{between F1 and F5,} \quad \tilde{J} = \frac{1 - \tilde{K}(1-\Delta^2)}{1+\Delta}, \\
&\text{between F1 and FR2,} \quad \tilde{J} = 1, \\
&\text{between FR2 and F5,} \quad \tilde{J} = \frac{1 + \tilde{K}(1-\Delta^2)}{1-\Delta},
\end{aligned} \tag{21}$$

$$\text{between F5 and FR1,} \quad \tilde{J} = \frac{2\Delta - 1 + \Delta(1+\Delta)(1+2\Delta)\tilde{K} + [1 + \Delta(1+\Delta)\tilde{K}]\sqrt{1+8\Delta^2}}{2\Delta(1+\Delta)}; \tag{22}$$

here $\tilde{J} = J/J_0$ and $\tilde{K} = K/J_0$.

IV. EXACT SOLUTION AND THERMODYNAMICS

The present model could be solved exactly using the known decoration transformation earlier presented by M. E. Fisher,[20,21] and recently generalized for arbitrary spin interactions,[22] where one maps the partition function of the system to the partition function of a one-dimensional Ising model, writing the relations for the entries of the transfer matrix and thus obtaining the relations between model parameters and that of an Ising chain. But here we implement a direct transfer matrix calculation without any account of the solution of an Ising chain. Therefore let us consider the following partition function of the system, which can be represented as

$$\begin{aligned}
\mathcal{Z} &= \sum_{\sigma} \mathrm{Sp_S} \exp(-\beta\mathcal{H}) \\
&= \sum_{\sigma} \prod_{i=1}^{N} \exp\left[\beta\frac{h_2}{2}(\sigma_i + \sigma_{i+1})\right] Z(\sigma_i,\sigma_{i+1}),
\end{aligned} \tag{23}$$

where β as usual is inverse temperature and the *partial* partition function for one dimer is introduced:

$$\begin{aligned}
Z(\sigma_i,\sigma_{i+1}) &= \mathrm{Sp}_i \exp(-\beta\mathcal{H}_i) \\
&= \sum_{n=1}^{9} \exp[-\beta\lambda_n(\sigma_i,\sigma_{i+1})].
\end{aligned} \tag{24}$$

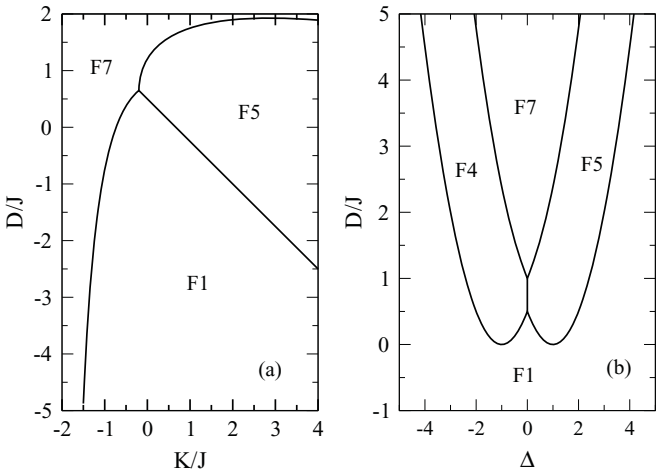

FIG. 4. Ground-state phase diagrams demonstrating the effect of single-ion anisotropy. Here $h = 1$, $j_0 = 1$. (a) The ground-state phase diagram in the (κ, δ) plane for a fixed value of exchange anisotropy $\Delta = 1/2$; (b) the ground-state phase diagram in the (Δ,δ) plane for a fixed value of biquadratic interaction $\kappa = 1/2$.

At this stage one can easily observe that the structure of the system implies the possibility of introducing the decoration-iteration transformation;[20,22] however, we prefer to perform a direct transfer matrix calculation.[25–28]

Then, the *partial* partition function (24) corresponding to one block can be easily expressed in the following form:

$$Z(\sigma_i,\sigma_{i+1}) = \sum_{n=0}^{2} Z_n \cosh\{\beta n[h_1 - J_0(\sigma_i + \sigma_{i+1})]\},$$
$$Z_0 = e^{\beta(J-K-2D)} + 2e^{\beta\frac{1}{2}[J-(1+4\Delta^2)K-2D]}\cosh\left(\frac{\beta R}{2}\right),$$
$$Z_1 = 4e^{-\beta(\Delta K+D)}\cosh(\beta\Delta J), \qquad (25)$$
$$Z_2 = 2e^{-\beta(J+K+2D)}.$$

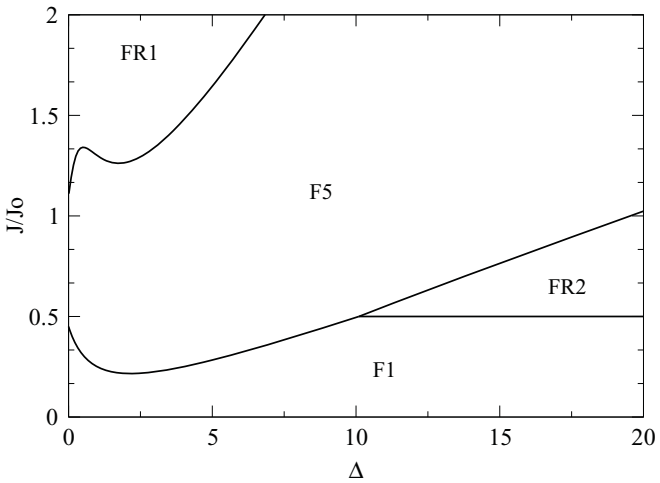

FIG. 5. Zero-field ground-state phase diagram drawn in the $(\Delta, J/J_0)$ plane for fixed $D = 0$ and small values of $K/J_0 = 0.1$. The frustrated ground states are exhibited.

After that, one can represent the partition function (23) in a similar form to the partition function of a chain with classical two state variables on each site:

$$\mathcal{Z} = \sum_{\sigma}\prod_{i=1}^{N} T(\sigma_i,\sigma_{i+1}) = \mathrm{Sp}\mathbf{T}^N = \Lambda_1^N + \Lambda_2^N, \qquad (26)$$

where $\Lambda_{1,2}$ are two eigenvalues of the transfer-matrix $\mathbf{T}$, which takes the following form:

$$\mathbf{T} = \begin{pmatrix} e^{\beta\frac{h_2}{2}}\mathcal{Z}_+ & \mathcal{Z}_0 \\ \mathcal{Z}_0 & e^{-\beta\frac{h_2}{2}}\mathcal{Z}_- \end{pmatrix}, \qquad (27)$$

where

$$\mathcal{Z}_\pm = Z(\pm 1/2, \pm 1/2),$$
$$\mathcal{Z}_0 = Z(1/2, -1/2) = Z(-1/2, 1/2). \qquad (28)$$

Then, calculating the eigenvalues and taking thermodynamic limit, when only the largest eigenvalue survives, one arrives at the following expression for the free energy per block:

$$f = -\frac{1}{\beta}\log\left\{\frac{1}{2}\left[e^{\beta\frac{h_2}{2}}\mathcal{Z}_+ + e^{-\beta\frac{h_2}{2}}\mathcal{Z}_- + \sqrt{(e^{\beta\frac{h_2}{2}}\mathcal{Z}_+ - e^{-\beta\frac{h_2}{2}}\mathcal{Z}_-)^2 + 4\mathcal{Z}_0{}^2}\right]\right\}. \qquad (29)$$

As soon as the free energy per block is calculated, one can obtain analytic expressions for all thermodynamic function.

A. Magnetization and quadrupole moment

Magnetic quantities can be obtained using the free-energy expression obtained in (29). Therefore the magnetization of the spin S can be expressed as

$$M_S = \frac{1}{2N\mathcal{Z}}\sum_{\sigma}\mathrm{Sp}_S\left[\sum_{i=1}^{N}(S_{i1}^z + S_{i2}^z)e^{-\beta\mathcal{H}}\right] = -\frac{1}{2}\left(\frac{\partial f}{\partial h_1}\right)_{\beta,h_2,D}, \qquad (30)$$

while the magnetization of spin σ reads as

$$M_\sigma = \frac{1}{N/2\mathcal{Z}}\sum_{\sigma}\mathrm{Sp}_S\left(\sum_{i=1}^{N}\sigma_i e^{-\beta\mathcal{H}}\right) = -2\left(\frac{\partial f}{\partial h_2}\right)_{\beta,h_1,D}. \qquad (31)$$

Thus the total magnetization is given by

$$M = \tfrac{1}{5}M_\sigma + \tfrac{4}{5}M_S. \qquad (32)$$

Figure 6(a) displays the plot of magnetization as a function of biquadratic interaction term K in units of J, for fixed values of $H/J = 3$, $T/J = 0.15$, $\Delta = 2$, and $J_0/J = 0.5$. Here one can see the plateaus for different values of J; these plateaus occur as expected at $1/5$ and $3/5$. The plots of magnetization processes (M versus H) for the system under consideration are presented in Fig. 6(b). Here the values of parameters are fixed as $K/J = 0.5$, $T/J = 0.15$, $\Delta = 1$, and the value of D/J varies from -1 to 1. Here we show two plateaus at 0.2 and 0.6. Thermal behavior of magnetization at the fixed external field is presented in Fig. 6(c), where the following values of parameters are assumed: $H/J = 4$, $\Delta = 1.4$, $D/J_0 = 1$,

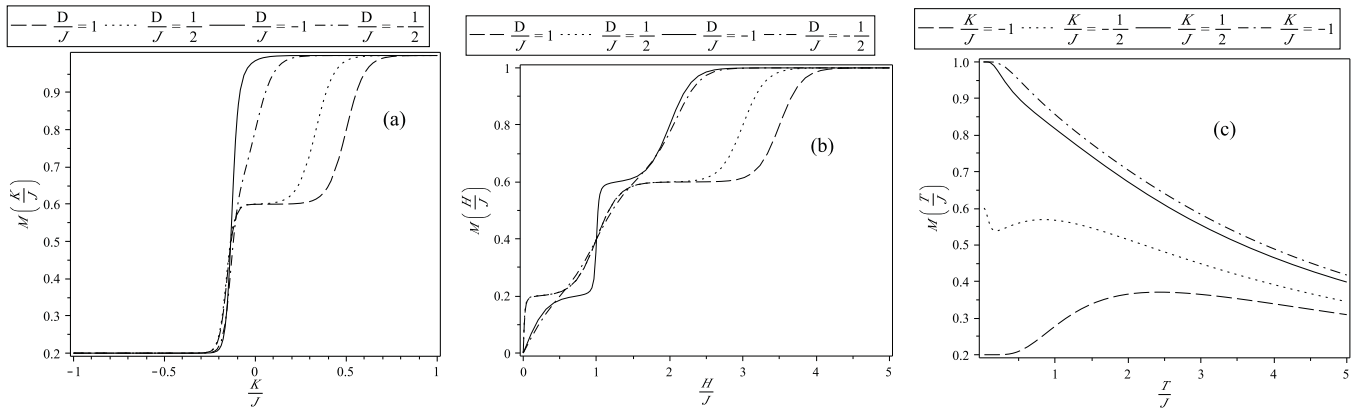

FIG. 6. (a) Magnetization as a function of K/J, for $H/J = 3.0$, $T/J = 0.15$, $\Delta = 2$, and $J_0/J = 0.5$. (b) Magnetization as a function of H/J, for $K/J = 0.5$, $T/J = 0.15$, $\Delta = 1$, and $J_0/J = 0.5$. (c) Magnetization versus temperature T/J, for $J_0/J = 0.5$, $H/J = 4$, $\Delta = 1.4$, and $D/J = 1$.

and $J_0/J = 0.5$, where we display the competition effect between ferromagnetic state SP and ferrimagnetic state F1 with magnetization $M = 3/5$, when temperature increases. Close to zero temperature one obtains three well-defined values for the magnetization, which are in accordance with plateaus displayed in Fig. 6(a) and 6(b).

As the system under consideration contains sites with spin-1 one can define another important physical quantity, the quadrupole moment, which can be obtained by the thermodynamic relations as well:

$$Q = \frac{1}{2N\mathcal{Z}} \sum_{\sigma} \mathrm{Sp_S} \left\{ \sum_{i=1}^{N} \left[\left(S_{i1}^{z}\right)^2 + \left(S_{i2}^{z}\right)^2 \right] e^{-\beta\mathcal{H}} \right\} = \frac{1}{2} \left(\frac{\partial f}{\partial D} \right)_{\beta,h_1,h_2}. \quad (33)$$

Some properties of the quadrupole moment also will be discussed due to the contribution of the biquadratic and uniaxial single-ion anisotropy parameters.

In Fig. 7(a) the plots of the quadrupole moment as a function of K/J for fixed values of $H/J = 3$, $J_0/J = 0.5$, $\Delta = 2$, and $T/J = 0.15$ are presented for several temperatures. The nontrivial and nonmonotone behavior of Q under variation of K can be understood if one takes into account the appearance of F7 and FR2 ground states in which the vertical quantum dimer is in an $|v_{0,-}\rangle$ eigenstate. Calculating the expectation value for the operator Q for this state one obtains

$$\langle v_{0,-}|\frac{1}{2}\left[\left(S_1^z\right)^2 + \left(S_2^z\right)^2\right]|v_{0,-}\rangle = \frac{1}{1 + \frac{1}{8\Delta^2}\left(1 + \frac{2D-R}{K-J}\right)^2}, \quad (34)$$

which actually defines the low-temperature behavior of the quadrupole moment. The quadrupole moment dependence of the uniaxial single-ion anisotropy parameter D is illustrated in Fig. 7(b), assuming $H/J = 2$, $J_0/J = -0.5$, $T/J = 0.1$, and $\Delta = 2$. Similar to the case of the magnetization we obtain some plateaus, but for higher values of D we have a decreasing curve instead of plateaus (solid line). On the other hand, as soon as the temperature increases, these plateaus obviously disappear. In Fig. 7(c) we plot the quadrupole moment as a function of the temperature for fixed values of $J_0/J = 0.5$, $D/J = 1.0$, $H/J = 4$, and $\Delta = 1.4$, similar to the case of magnetization [Fig. 6(c)], where the quadrupole moment leads to fixed values at low temperature, which are related to the plateaus displayed in Fig. 7(a) and 7(b), while at high temperature the average quadrupole moment leads to $2/3$, which corresponds to equal probabilities for all three values of $S = 1$ spin.

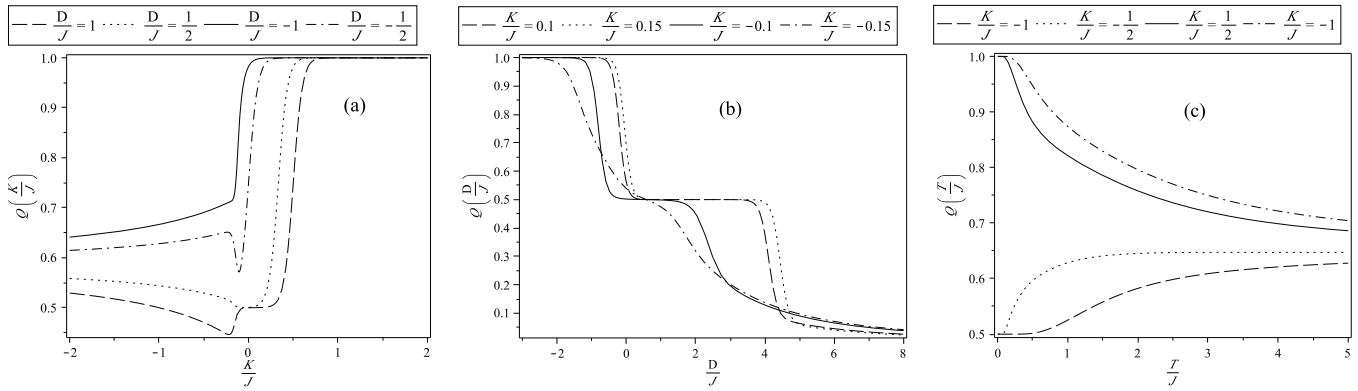

FIG. 7. Quadrupole moment: (a) As a function of K/J, for $H/J = 3$, $J_0/J = 0.5$, $\Delta = 2$, and $T/J = 0.15$; (b) as a function of D, for $J/J_0 = -0.5$, $T/J = 0.1$, $H/J = 2$, and $\Delta = 2$; (c) as a function of T, for $J_0/J = 0.5$, $D/J = 1.0$, $H/J = 4$, and $\Delta = 1.4$.

V. CONCLUSION

We have considered an exactly solvable variant of a diamond chain with mixed $S = 1$ and $S = 1/2$ spins. The vertical $S = 1$ dimers are taken as quantum ones with Heisenberg interaction, biquadratic interaction, and single-ion anisotropy terms, while all interactions between $S = 1$ spins and $S = 1/2$ spins residing on the intermediate sites are taken in the Ising form. The system generalizes the model of diamond chain with Ising and Heisenberg bonds considered in Ref. 14. Our results supplement the previously obtained ones for the case of $S = 1$ vertical XXZ dimers with only bilinear Heisenberg interaction. Despite the common subject, the solution method used in the present paper is different from that of Ref. 14. The authors of Ref. 14 work with the decoration-iteration transformation,[20,21] mapping the partition function and thermal averages to the partition function and thermal averages of the Ising chain. Exploiting then the known exact results of an Ising chain and using numerical solutions of the decoration-iteration transformation relations they obtain the plots of various observables. The direct transfer matrix calculation used in the present paper allows us to avoid any numerics and provides a ground for direct physical intuition. One of the main goals of our research is to perform the detailed analysis of various $T = 0$ ground-state phase diagrams, in particular emphasizing biquadratic interaction and single-ion anisotropy effects. As the number of parameters in the considered model are rather high, the phase diagrams have been shown to be rather rich, demonstrating a large variety of ground states: saturated one, three ferrimagnetic ground states with magnetization equal to $3/5$, and four other ferrimagnetic ground states with magnetization equal to $1/5$. There are also two frustrated macroscopically degenerated ground states that exist at a zero magnetic filed. In general, depending on the values of parameters, the system can exhibit all ten ground states described in the paper, which is almost two times larger that in the $S = (1,1/2)$ Ising–Heisenberg diamond chain considered in Ref. 14. The thermodynamic properties of the model have been described exactly by exact calculation of partition function within the direct classical transfer-matrix formalism. The entries of transfer matrix, in their turn, contain the information about quantum ground states of the vertical $S = 1$ XXZ dimer (eigenvalues of local hamiltonian for vertical link). It is worth mentioning that the recent achievements in the synthesis of novel coordination polymer compounds containing highly anisotropic magnetic ions[32,33] make the research field of an exact solution of the Ising-Heisenberg spin chains not only interesting from the abstract statistical mechanics point of view, but also practically relevant for computation of the magnetic and thermodynamic properties of novel magnetic materials.

ACKNOWLEDGMENTS

VO expresses his gratitude to the Institut für Theoretische Physik Universität Göttingen for warm hospitality during the final stage of this work. This research stay was supported by DFG (Project No. HO 2325/7-1). VO and MK were partly supported by the joint grant of CRDF-NFSAT and the State Committee of Science of the Republic of Armenia No. ECSP-09-94-SASP. VO was also partly supported by the Volkswagen Foundation (Grant No. I/84 496) and ANSEF-1981-PS. OR and SMS thank CNPq and FAPEMIG for partial financial support.

*ors@dex.ufla.br
†ohanyan@yerphi.am

[1] F. Aimo, S. Krämer, M. Klanjŭsek, M. Horvatič, C. Berthier, and H. Kikuchi, Phys. Rev. Lett. **102**, 127205 (2009).
[2] K. C. Rule, A. U. B. Wolter, S. Süllow, D. A. Tennant, A. Brühl, S. Köhler, B. Wolf, M. Lang, and J. Schreuer, Phys. Rev. Lett. **100**, 117202 (2008).
[3] H. Kikuchi, Y. Fujii, M. Chiba, S. Mitsudo, T. Idehara, T. Tonegawa, K. Okamoto, T. Sakai, T. Kuwai, and H. Ohta, Phys. Rev. Lett. **94**, 227201 (2005).
[4] B. Gu and G. Su, Phys. Rev. B **75**, 174437 (2007).
[5] K. Hida, K. Takano, and H. Suzuki, J. Phys. Soc. Jpn. **78**, 084716 (2009).
[6] K. Takano, H. Suzuki, and K. Hida, Phys. Rev. B **80**, 104410 (2009).
[7] T. Sakai, K. Okomoto, and T. Tonegawa, J. Phys. Conf. Series **200**, 022052 (2010).
[8] N. B. Ivanov, J. Richter, and J. Schulenburg, Phys. Rev. B **79**, 104412 (2009).
[9] H. H. Fu, K. L. Yao, and Z. L. Liu, Phys. Rev. B **73**, 104454 (2006).
[10] M. S. S. Pereira, F. A. B. F. de Moura, and M. L. Lyra, Phys. Rev. B **77**, 024402 (2008).
[11] M. S. S. Pereira, F. A. B. F. de Moura, and M. L. Lyra, Phys. Rev. B **79**, 054427 (2009).
[12] O. Derzhko, A. Honecker, and J. Richter, Phys. Rev. B **79**, 054403 (2009).
[13] J. S. Valverde, O. Rojas, and S. M. de Souza, Physica A **387**, 1947 (2008).
[14] L. Čanová, J. Strečka, and M. Jaščur, J. Phys. Condens. Matter **18**, 4967 (2006).
[15] L. Čanová, J. Strečka, and T. Lučivjanský, Condens. Matter Phys. **12**, 353 (2009).
[16] J. Strečka, L. Čanová, T. Lučivjanský, and M. Jaščur, J. Phys. Conf. Series **145**, 012058 (2009).
[17] H. Kobayashi, Y. Fukumoto, and A. Oguchi, J. Phys. Soc. Jpn. **78**, 074004 (2009).
[18] T. A. Arakelyan, V. R. Ohanyan, L. N. Ananikyan, N. S. Ananikian, and M. Roger, Phys. Rev. B **67**, 024424 (2003).
[19] T. Verkholyak, J. Strečka, M. Jaščur, and J. Richter, e-print arXiv:1004.0848 (2010).
[20] M. E. Fisher, Phys. Rev. **113**, 969 (1958).
[21] I. Syozi, *Phase Transitions and Critical Phenomena*, Vol. 1, edited by C. Domb and M. S. Green (Academic Press, New York, 1972), p. 269.
[22] O. Rojas, J. S. Valverde, and S. M. de Souza, Physica A **388**, 1419 (2009).
[23] J. S. Valverde, O. Rojas, and S. M. de Souza, J. Phys. Condens. Matter **20**, 345208 (2008).

[24]V. Hovhannisyan and N. Ananikian, Phys. Lett. A **372**, 3363 (2008).
[25]D. Antonosyan, S. Bellucci, and V. Ohanyan, Phys. Rev. B **79**, 014432 (2009).
[26]V. Ohanyan, Phys. Atomic Nucl. **73**, 494 (2010).
[27]V. Ohanyan, Condens. Matter Phys. **12**, 343 (2009).
[28]S. Bellucci and V. Ohanyan, Eur. Phys. J. B **75**, 531 (2010).
[29]J. Strečka, M. Jaščur, M. Hagiwara, Y. Narumi, K. Kindo, and K. Minami, Phys. Rev. B **72**, 024459 (2005).
[30]V. Ohanyan and N. Ananikian, Phys. Lett. A **307**, 76 (2003).
[31]F. Litaiff, J. Desousa, and N. Branco, Solid State Commun. **147**, 494 (2008).
[32]D. Visinescu, A. M. Madalan, M. Andruh, C. Duhayon, J.-P. Sutter, L. Ungur, W. Van der Heuvel, and L. F. Chibotary, Chem. Eur. J. **15**, 11808 (2009).
[33]W. Van den Heuvel and L. F. Chibotaru, Phys. Rev. B **82**, 174436 (2010).
[34]C. Kittel, Phys. Rev. **120**, 335 (1960).
[35]R. Baxter, *Exactly Solved Models in Statistical Mechanics* (Academic Press, New York, 1982).